Proven Sensor Performance for Emerging Shock Environments

Vesta I. Bateman, Mechanical Shock Consulting, Albuquerque, New Mexico
James Letterneau, Meggitt Sensing Systems, Orange County, California

There are new shock regimes that are emerging for existing threat environments. These shock environments have not yet appeared in standards, but they will appear soon. These new shock environments are created by an improvised explosive device (IED), often used in unconventional warfare. Wideband (1 MHz) field data demonstrate the survivability of the Endevco® 7280A in addition to showing that its damped resonance does not interfere with measuring a severe, combined shock environment consisting of a near-field ballistic shock combined with a shock-induced velocity change. To further characterize the performance of the damped accelerometer, a series of full-range, short-duration, Hopkinson bar testing has been conducted at the Meggitt Sensing Systems shock laboratory with a laser Doppler vibrometer (LDV) as the reference measurement. Performance characteristics discussed include time domain amplitude linearity and frequency domain characteristics that are compared to the characteristics of the industry-standard undamped 7270A accelerometers. Additionally, it is shown that these accelerometers meet the new *MIL-STD-810G, Change Notice 1* requirements for calibration.

Meggitt Sensing Systems (MSS) has developed a family of lightly damped, high-g shock accelerometers, the Endevco® 7280A, which are available in various legacy package configurations in both 20,000-g and 60,000-g ranges. This MEMS-based (silicon), piezoresistive (PR), high-g shock accelerometer incorporates light gas damping and mechanical over-travel stops that have demonstrated survivability and reliability in harsh and unpredictable environments.

Previous literature has discussed amplitude linearity to one and one-half times the specified range (minimum), flat frequency response (±5%) to 10,000 Hz, shock survivability to four times the specified range, minimum zero shift aftershock as well as the trade-off between gas damping and resonant frequency.[1-6] The legacy package is shown in Figure 1 with the modal frequencies for the 7280A. This MEMS-damped accelerometer is also available in other legacy packages that are part of the Endevco® family of high-g shock accelerometers: 7280AM4 (1/4-inch, 28 mounting stud, extensively studied)[7], 72 (surface mount package) and 7284 (triaxial, bolt mount).

Before the introduction of the 7280A,[8] the only commercially available piezoresistive option for measurements in harsh environments was the Endevco 7270AM6, which was a mechanically filtered version of the Endevco 7270A undamped high-shock accelerometer. The 7270AM6 was developed by Sandia National Laboratories[9] in Albuquerque, NM, and made commercially available by Endevco Corporation (now Meggitt Sensing Systems).

Before the development of lightly damped piezoresistive shock sensors, the mechanically filtered 7270AM6 served as an interim solution to obtain valid data for nuclear weapons delivery environments and other components and systems over a wide bandwidth. In comparison to the 7270A, the 7270AM6 is a more robust solution, because it utilizes mechanical isolation of the undamped resonance of the 7270A that caused breakage in high velocity applications. While the 7270AM6 performed well as an interim solution, the ultimate solution is the Endevco 7280A, a lightly damped, high-g shock accelerometer.

The 7280A design is made possible with the lightly damped MEMS sensing element designed and manufactured at Meggitt's silicon fab (semiconductor fabrication plant) in Sunnyvale, CA. The development initiated over a decade ago, and the first patent was granted to Bruce Wilner in 2006.[1-6] Bruce Wilner is the inventor of the MEMS sensing elements used in the Endevco 7270A, including the world's first and only 200,000-g accelerometer (1971), and now the 7280A (plus many more not mentioned here).

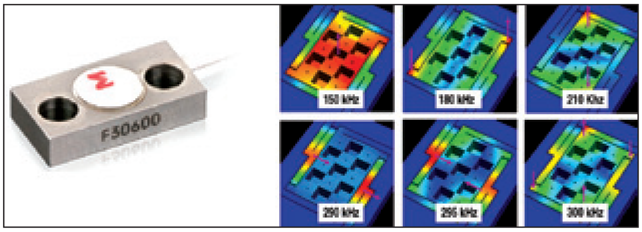

Figure 1. Endevco 7280A legacy packaging (left) and modal frequencies.

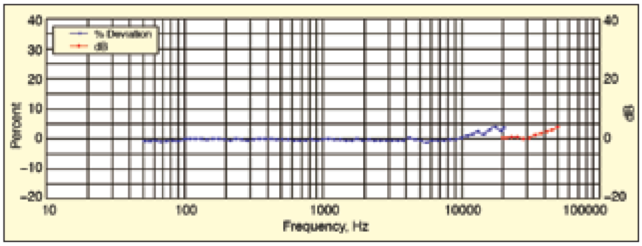

Figure 2. Sample vibration calibration for Endevco® 7280A-20K (18.56 µV/g @ 100 Hz, 10 g peak).

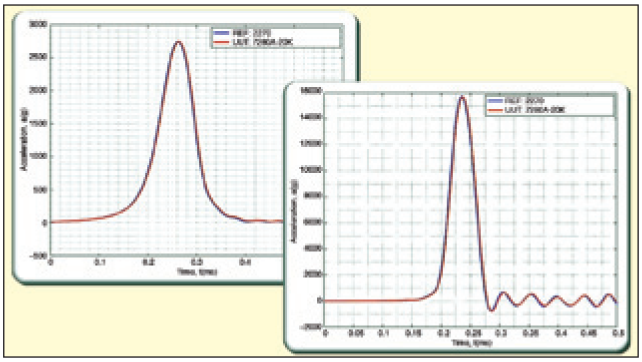

Figure 3. Sample shock time domain calibration, Endevco 7280A-20K.

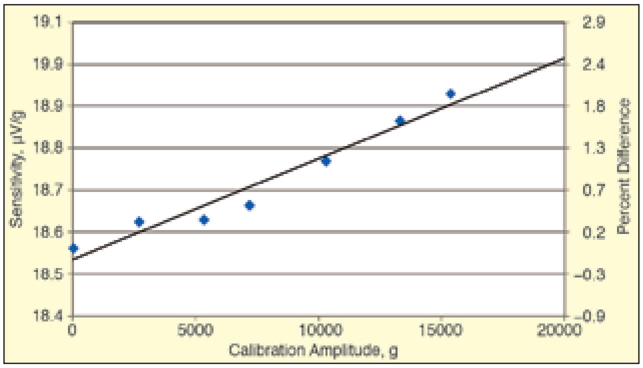

Figure 4. Full-range shock calibration, Endevco 7280A-20K.

This article consists of three evaluations: shock and vibration calibration results, full-range Hopkinson bar evaluations, and field data results for a severe, combined shock environment of near-field ballistic shock combined with a shock-induced velocity change and is an update to the previous article with similar evaluations but with a laser Doppler vibrometer as the reference measurement.[8]

Shock and Vibration Calibration Results

Figure 2 shows a sample vibration calibration 7280A-20K. Note that swept-sine vibration calibrations are not typically performed on high-shock accelerometers due to the low signal-to-noise ratio of the test. (The test is run at 10 g, which is 0.05% full scale output.) For the data presented, there are two scales: one for 50 to 20,000 Hz (left, in percent) and one for 20,000 to 50,000 Hz (right, in dB). On the specific unit tested, the response is within ±5% from 50 to 20,000 Hz; the typical specification for the 7280A is ±5% to 10 kHz and 13 kHz for the 7280A-20K and 7280A-60K, respectively.

Figure 3 shows two time-domain comparisons of the 7280A-20K and the 2270, which is the industry-standard reference transducer for shock calibration. The time-domain comparisons have identical time-domain response between the two accelerometers. The after pulse ringing at about 1600 g reflects the structural response of the shock-generating apparatus and is present on both the reference accelerometer and the unit under test (UUT). The final overall calibration in Figure 4 has both vibration calibration data at 10 g as well as full range shock sensitivity with a percent deviation of ~2.5%.

The calibration data shown here meet the new calibration requirements that now appear in *MIL-STD-810G, Change Notice 1*[10] (released April 2014), Method 516, for Shock, and Method 517 for Pyroshock. These requirements include a frequency-domain requirement and a time-domain requirement for calibration. The frequency-domain requirement is: *A flat frequency response within ±5 percent across the frequency range of interest is required. Since it is generally not practical or cost effective to conduct a series of varying pulse width shock tests to characterize frequency response, a vibration calibration is typically employed.*

The time domain requirement is: *If the sensitivity is based upon the low amplitude vibration calibration, it is critical that the linearity characteristics of the shock based "Amplitude Linearity" be understood such that an amplitude measurement uncertainty is clearly defined. Ideally, vibration calibration and shock amplitude linearity results should agree within 10 percent over the amplitude range of interest for a given test.*

In addition, Sandia National Laboratories has an internal requirement, in effect for more than 40 years that requires the accelerometer sensitivities determined by both vibration and shock calibrations to agree within 8%. Clearly, the Endevco 7280A already meets these requirements (as well as Endevco's 7270A for more than 25 years). There are many shock accelerometers that cannot and will not meet these requirements, because their performance is based on 10 g vibration calibrations alone.

Full-Range Hopkinson Bar Evaluations

Why use a Hopkinson bar instead of low-level vibration calibrations or relatively low-level, drop-ball shock calibrations? Typically, a Hopkinson bar provides the widest bandwidth frequency domain information at shock peak amplitudes. A Hopkinson bar evaluation may excite the transducer resonance depending on the pulse duration that is governed by the geometry and material for the bar. Certainly, real shock/pyroshock environments will excite the transducer resonance in most situations.

Hopkinson bar evaluations can reveal a more realistic prediction of transducer response in actual use compared to low-level calibration methods. Table 1 shows the initial test matrix for full range Hopkinson bar evaluations. The Hopkinson bar, also known as Kolsky or Davies bar configuration,[12,13] is shown in Figure 5. The evaluations here use a new reference measurement, a Polytec laser Doppler vibrometer (LDV) that has an assigned uncertainty of ±3%[14] for this Hopkinson bar configuration, where the bar's rigid body motion after the shock moves towards the LDV.

Table 1. Test plan for 7280A full-range Hopkinson bar evaluations.

Accelerometer	Peak Shock Levels	Number of Impacts
Endevco 7280A-20K	10, 20 and 30	5
Endevco 7280A-60K	30, 60 and 89	5

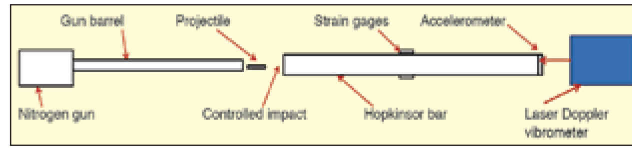

Figure 5. Typical single, Hopkinson bar configuration for full-range Hopkinson bar evaluations with laser Doppler vibrometer reference measurement.

The Hopkinson bar configuration used in this test series underwent numerous upgrades compared to the previous configuration, which was not suitable for the LDV reference measurement. Specifically, the base structure and bar mounting were adjusted so that the bar and LDV remain in constant alignment throughout the test, since any misalignment results in a dropped signal on the LDV. Also relating to alignment, the Hopkinson bar control panel was decoupled from the bar mounting structure to ensure alignment is maintained while operating the controls. A new nitrogen gas reservoir was selected to release pressure more quickly and minimize the frictional effects that reduce the available nitrogen pressure needed to create high-velocity, short-duration projectile impacts of the Hopkinson bar. Finally, different programming (pulse shaping) techniques were used to create repeatable, shorter pulses.

The theory of stress wave propagation in a Hopkinson bar is well documented.[12,13] The bar material is 6AL-4V titanium alloy (6% aluminum and 4% vanadium) with a diameter of 0.625 inch and bar length of 5 feet. A Hopkinson bar is defined as a perfectly elastic homogeneous bar of constant cross-section. A stress wave will propagate in a Hopkinson bar as a one-dimensional elastic wave without attenuation or distortion if the wavelength λ is large relative to the radius a or:

$$\lambda > 10a \tag{1}$$

Also, the longitudinal (extensional) wavelength approaches infinity for length/radius ratio>20. For a one-dimensional stress wave propagating in a Hopkinson bar, the motion of a free end of the bar as a result of this wave is:

$$V = 2C_0\varepsilon \tag{2}$$

or

$$a = 2C_0\frac{d\varepsilon}{dt} \tag{3}$$

where

$$C_0 = \sqrt{\frac{E}{\rho}} \tag{4}$$

and v and a are the velocity and acceleration, respectively, of the end of the bar; c_o is the nominal wave propagation speed in the bar based on material properties; E is the modulus of elasticity, r is the density for the Hopkinson bar material, and ε is the strain measured in the bar at a location that is not affected by reflections during the measurement interval.

Titanium is a good material for an everyday Hopkinson bar, because for a given stress σ the measured strain ε from the strain gages will be higher if the modulus of elasticity is lower. An additional reference measurement is made with strain gages mounted diametrically opposed at the midpoint of the bar; the strain gages have an assigned uncertainty of +6%.[15] The motion of an accelerometer mounted on the end of the bar will be governed by Equations 2 and 3 if the mechanical impedance of the accelerometer is much less than that of the bar or if the thickness of the accelerometer is much less than the wavelength. The requirement on the strain gage is that the gage length (g.1) be much less than the wavelength or $\lambda \geq (10 \times \text{g.1})$.

An overlay of the LDV time-domain results of five impacts digitally filtered with a Butterworth filter and a cutoff frequency of 100,000 Hz (filtered forward and backward to remove nonlinear phase) are shown in Figure 6, and the corresponding Fourier transforms are in Figure 7. These are 40 µs pulses that meet *MIL-STD-810G, Change Notice 1*[10]; additionally, the shock pulse duration for the evaluations is calculated as:

$$T_D = \frac{1}{2f_{\max}} \tag{5}$$

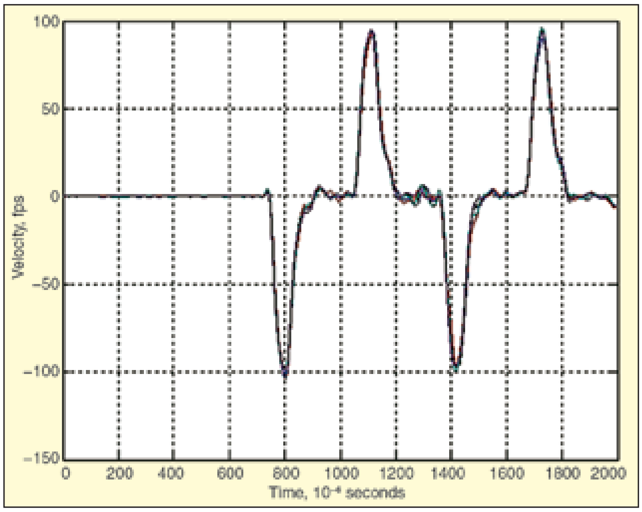

Figure 6. Overlay of LDV five impacts digitally filtered with cut-off frequency of 100,000 Hz.

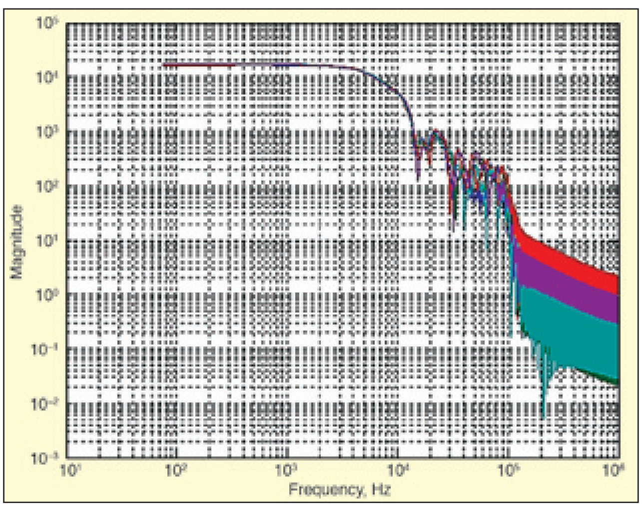

Figure 7. Fourier transforms corresponding to Figure 6.

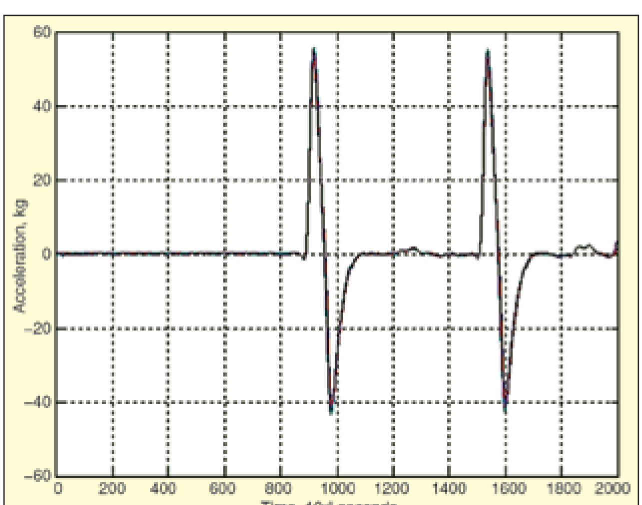

Figure 8. Overlay of 7280A five impacts digitally filtered with cut-off frequency of 100,000 Hz.

where T_D is the duration (baseline) of the acceleration pulse and f_{max} is the maximum specified frequency range for the accelerometer. For near-field pyroshock, f_{max} is 100,000 Hz. For mid-field and far-field pyroshock, f_{max} is 10,000 Hz. If Hopkinson bar testing is used for these evaluations then care must be taken to make sure that a nondispersive pulse duration is used.[11,15]

The 7280A measurements for these same input pulses and digitally filtered per above are shown in Figure 8, and the cor-

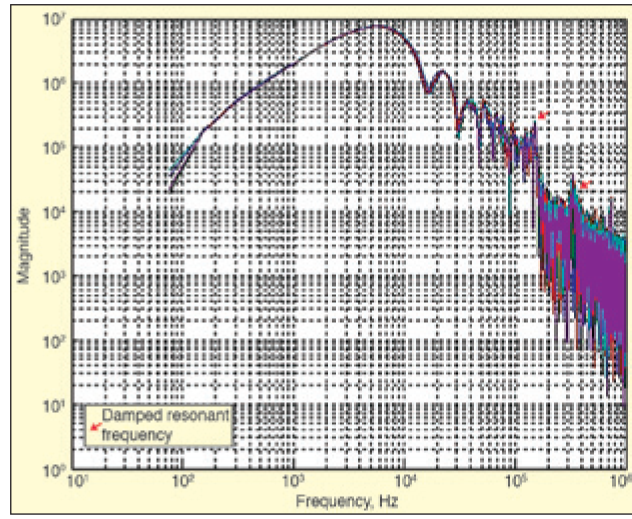

Figure 9. Fourier transforms corresponding to Figure 8.

responding Fourier transforms are in Figure 9. The noncausal effect of the digital filter[16] is evident in Figures 6 and 8. Since it is desired to preserve the frequency response of the data, acceleration is used for comparing the data. Consequently, the time derivative of the LDV records was required, and the resulting signal may be contaminated by high-frequency noise created in the process of calculating the derivative. This problem was essentially eliminated by adequate sample rate of 5 MHz, low-pass digital filtering with a cutoff frequency well above the frequency range of interest (100,000 Hz), and most importantly, an accurate differentiation algorithm derived from using the Fourier series reconstruction techniques.[17] This algorithm results in an exact derivative of the digitized signal, providing the sampling theorem has not been violated (data are not aliased).[16]

The complex frequency response function (FRF), $H(jw)$, gives amplitude and phase in the usual Equations 6-8.[18] Coherence is required for data where the performance of the input, x (reference measurement), relative to the output, y (accelerometer measurement), is unknown. Coherence is a measure of linearity or how does the output y relate to the input x as shown in Equation 9. The ideal coherence value is 1.0, and a coherence value less than ~0.90 is bad data:

$$H(j\omega) = \frac{H_1 + H_2}{2} \tag{6}$$

where:

$$H_1(jw) = \frac{\sum_{n=1}^{5} G_{xy}}{\sum_{n=1}^{5} G_{xx}} \tag{7}$$

and:

$$H_2(jw) = \frac{\sum_{n=1}^{5} G_{yy}}{\sum_{n=1}^{5} G_{yx}} \tag{8}$$

G_{xy} is the cross-spectrum between the reference LDV acceleration x and the accelerometer response y; G_{yx} is the cross-spectrum between the accelerometer response y and the reference LDV acceleration x; G_{yy} is the auto-spectrum of the accelerometer response y; and G_{xx} is the auto-spectrum of the LDV response. The FRF H_1 is biased by the error on the reference LDV acceleration, and the FRF H_2 is biased by the error on the accelerometer response. The Hopkinson bar data for these FRF calculations have noise on both the reference LDV acceleration and the accelerometer response, so the average of the two FRFs in Eq. 6 is used. The summations are performed for the ensemble of five reference accelerations and their corresponding accelerometer responses. The coherence, $\gamma^2_{xy}(jw)$, was also calculated for an ensemble of five data sets according to the equation:[18]

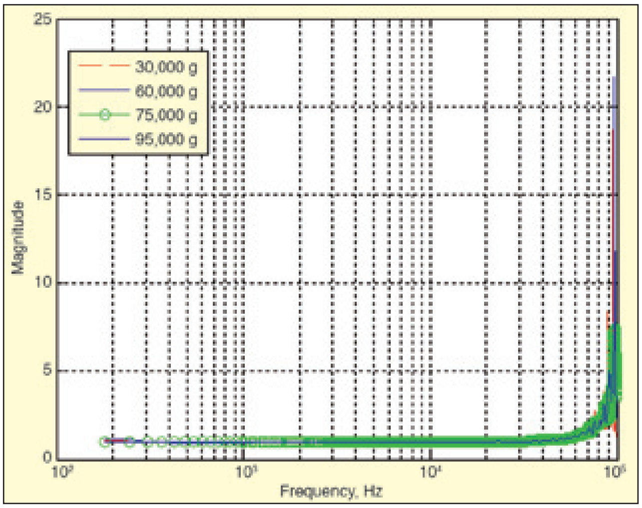

Figure 10. Legacy 7270A FRF magnitude with LDV reference measurement.

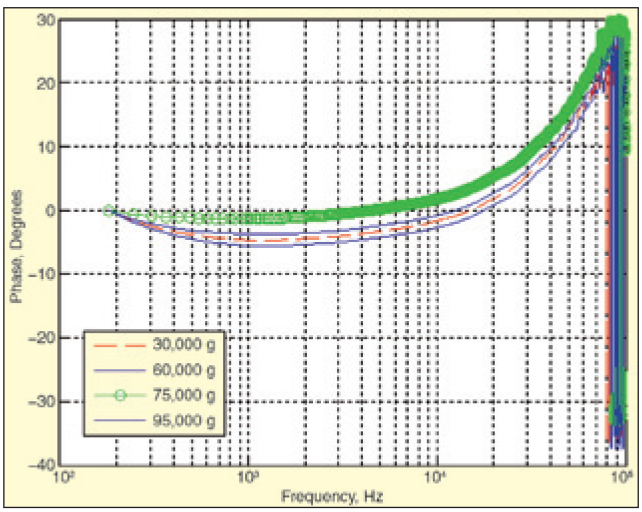

Figure 11. Legacy 7270A FRF phase with LDV reference measurement.

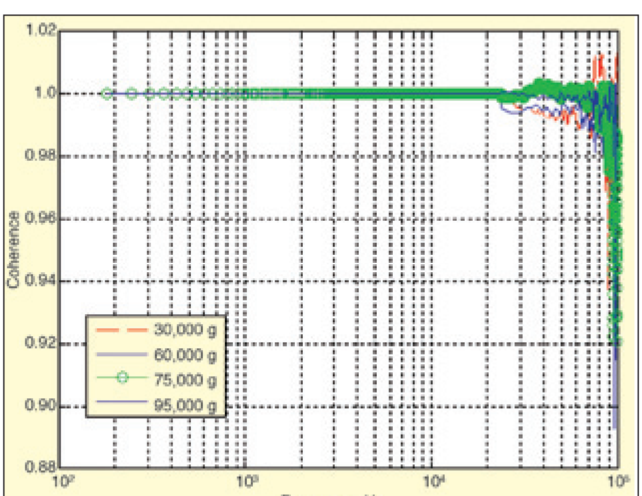

Figure 12. Legacy 7270A FRF coherence with LDV reference measurement.

$$\gamma_{xy}^{2}(jw) = \frac{H_1}{H_2} \tag{9}$$

as a measure of the linearity between the reference acceleration and the accelerometer response and of the noise in these data.

The FRF magnitude, phase, and coherence for the legacy sensor, the 7270A, are shown in Figures 10, 11 and 12, respectively. The FRFs show excellent performance for the 7270A-20K accelerometer. The pulse duration for this evaluation, 20 µs, yields a DC to 25 kHz nondispersive bandwidth for the titanium bar and meets

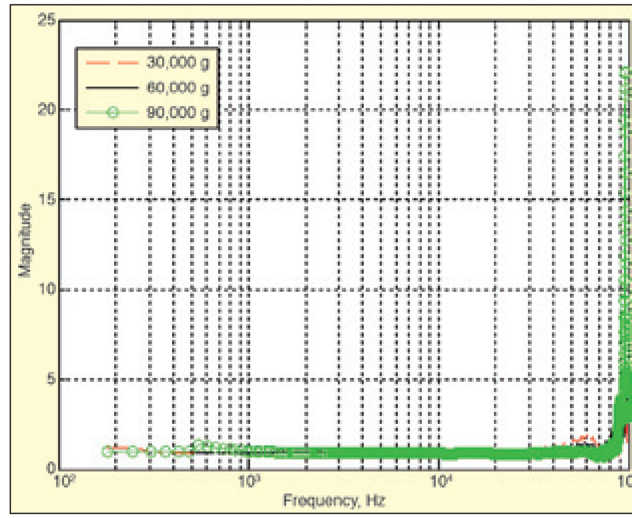

Figure 13. 7280A FRF magnitude with LDV reference measurement.

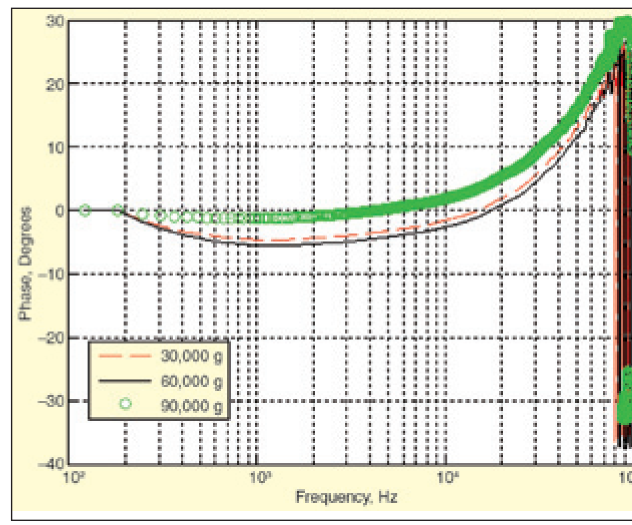

Figure 14. 7280A FRF phase with LDV reference measurement.

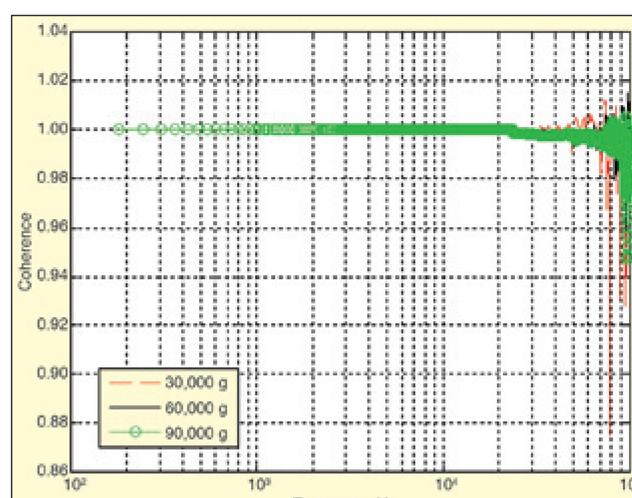

Figure 15. 7280A FRF coherence with LDV reference measurement.

MIL-STD-810G, Change Notice 1[10] requirements for pulse duration. The FRF for the 7280A magnitude, phase, and coherence are shown in Figures 13, 14 and 15. What is important about these data in Figures 10-15 is to note that the shock frequency domain performance is equivalent for the Endevco 7270A (legacy sensor) and the Endevco 7280A damped PR accelerometer.

Some explanation of Figures 10-15 is appropriate here. In shock testing how good or useful the data are is governed by coherence. In general, the coherence is a measure of how well the

Figure 16. Underbody blast environment – IED ignition.

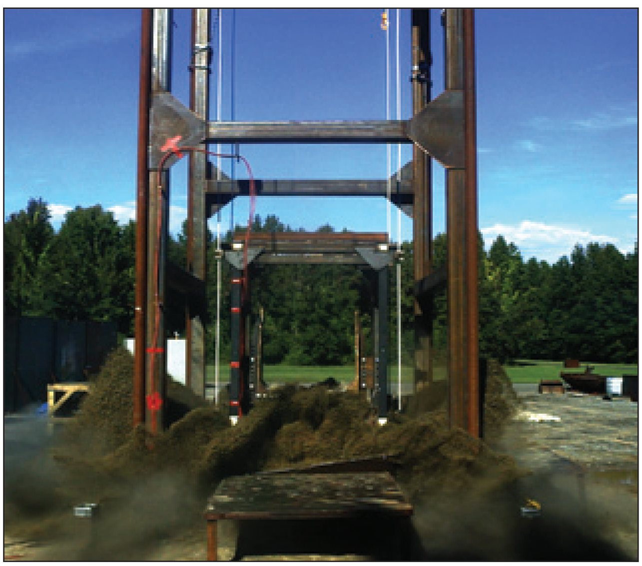

Figure 17. Underbody blast environment – simulated vehicle starts moving.

Figure 18. Underbody blast environment - simulated vehicle stops.

response of the unit under test, here the Endevco 7270A or the Endevco 7280A, represents the reference measurement, the laser Doppler vibrometer. A coherence value of 1.0 indicates a totally linear relationship between the unit under test and the reference

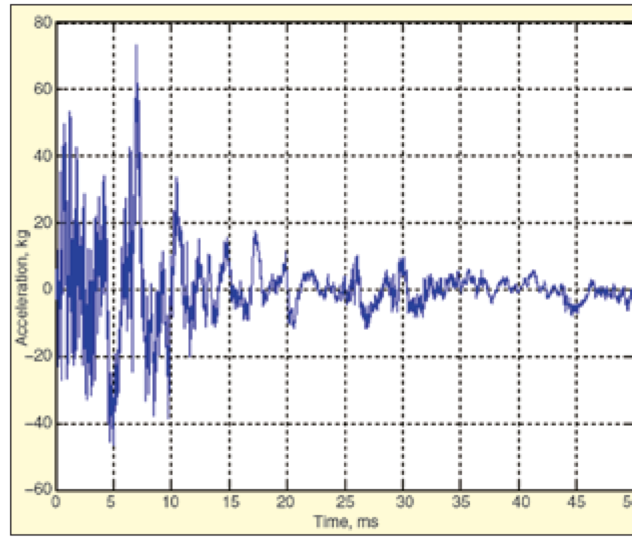

Figure 19. 7280A time-domain acceleration for severe, combined shock environment.

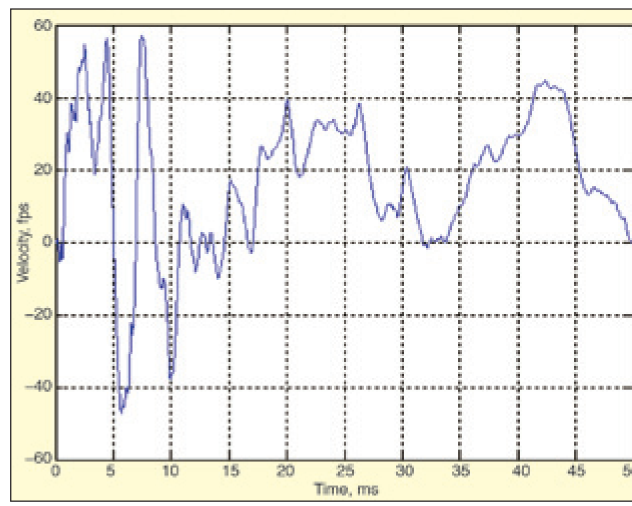

Figure 20. 7280A time-domain velocity for severe, combined shock environment.

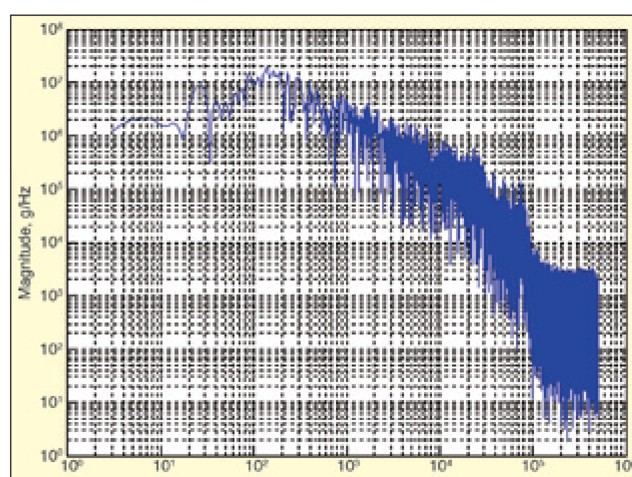

Figure 21. 7280A Fourier transform for severe, combined shock environment.

measurement. The purpose of calculating Frequency Response Functions (FRF) is to calculate three quantities – magnitude, phase and coherence. A coherence value of 0.99 or higher is considered good or useful data. Coherence of <0.90 is considered bad data, although this can be a judgement call. For example, if the data are difficult, time-consuming or expensive to obtain, someone who is analyzing the data might conclude that another, lower coherence value is acceptable.

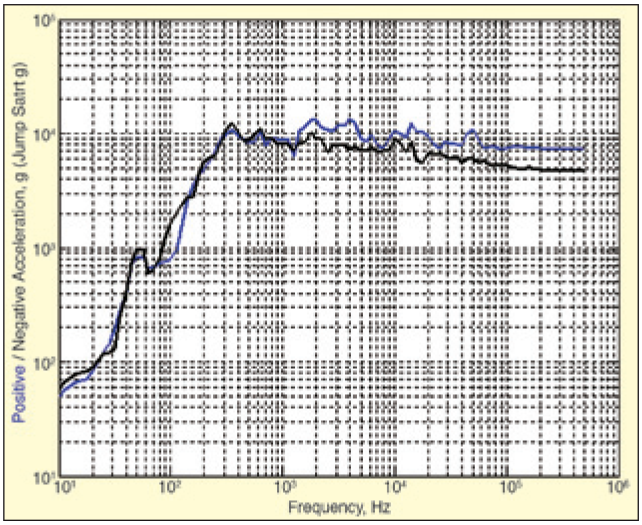

Figure 22. 7280A shock response spectra for severe, combined shock environment (Q=10).

For the purpose of interpretation of magnitude and phase for both the Endevco 7270A or the Endevco 7280A, the coherence is lost as shown in Figures 12 and 15 at 100 kHz, and the data are no longer useful above this frequency. The first resonance of the Endevco 7280A is 180 kHz, and there is no coherence at this frequency because for shock data, once coherence is lost, it is not regained. The plots show the loss of coherence, so that there is a clear indication of the frequency bandwidth of the data. The loss of coherence is also indicated by large deviations in magnitude and phase around 100 kHz. These deviations are not real but an artifact of the FRF calculation and limited bandwidth of the data.

Live Emerging Shock Environment Results

The proof of an accelerometer's performance cannot be fully accomplished with laboratory evaluations alone; actual field testing in real or simulated environments is also required. In this section, results are shown for the testing of the 7280A in a new, real and live emerging shock environment. A severe, combined shock environment of near-field pyroshock combined with a shock-induced velocity change was conducted with 2.5 kg of buried explosives. as shown in Figures 16-18.

This is the most difficult of events to measure to date and is an emerging shock environment. The Endevco 7280A-20K performed excellently, as shown in Figures 19-22. The acceleration time history appears to be an explosive classic, symmetric pyroshock with a velocity change as indicated by the positive offset. The quality of this acceleration measurement is confirmed by the velocity time history (integral of data in Figure 19) in Figure 20 that shows the rigid velocity change of ~60 fps plus the near-field pyroshock. The wideband Fourier transform in Figure 21 shows no effect of the first two damped resonances. All data in Figures 16-18 have a 1-MHz bandwidth that is appropriate for this severe, combined shock environment.

Finally, the shock response spectra (Q=10) in Figure 22 (calculated to 500,000 Hz) show the typical low-frequency slope starting at 10 Hz (9-12 dB/octave) and a lack of 1ow-frequency contamination from 10 Hz to 500 kHz. The shock response peaks above 10,000 Hz are common for near-field pyroshock with live explosives. The effect of the damped resonance of the 7280A accelerometer does not affect the shock response spectra below 500,000 Hz. There has been no manipulation of the data other than to remove the mean, which is a standard analysis technique.

Summary and Conclusions

A damped piezoresistive accelerometer, the Endevco 7280A, is in production and in field use. The proof of an accelerometer's performance cannot be achieved in laboratory evaluations alone, but real, live field testing in severe shock environments is also required, specifically the new emerging shock environments shown in this article.

The 7280A, offered in both 20,000 g and 60,000 g ranges, has a linear response in the time and frequency domains meeting the requirements of *MIL-STD-810G, Change Notice 1*. Full-range Hopkinson bar data show linear response in the frequency domain for coherent frequency response functions in the range of DC to 25,000 Hz as shown by FRFs. The 7280A damped resonances do not interfere with the measurement of a severe pyroshock environment, as shown by the live emerging shock environment data.

Acknowledgements

Carroll Barbour was instrumental in performing the Hopkinson bar test program at the Meggitt Sensing Systems Shock Laboratory in Orange County, CA.

References

1. T. Kwa, G. Pender, J. Letterneau, K. Easler, and R. Martin, "A New Generation of High-Shock Accelerometers with Extreme Survivability Performance," *Proc. 53rd NDIA Fuze Conference*, Lake Buena Vista, FL, May 21, 2009.
2. R. Martin, G. Pender, T. Kwa, J. Letterneau, and K. Easler, "High-Survivability, High-Shock Accelerometer," *Proc. 80th SAVIAC Shock and Vibration Symposium*, San Diego, CA, October 25-29, 2009.
3. L. B. Wilner, Meggitt Sensing Systems, San Juan Capistrano, CA, January 24, 2006, U.S. Patent No. 6,988,412; Piezoresistive strain concentrator, Washington, DC, U.S. Patent and Trademark Office.
4. L. B. Wilner, Meggitt Sensing Systems, San Juan Capistrano, CA, December 12, 2006, U.S. Patent No. 7,146,865; Piezoresistive strain concentrator, Washington, DC, U.S. Patent and Trademark Office.
5. L. B. Wilner, Meggitt Sensing Systems, San Juan Capistrano, CA, July 1, 2008, U.S. Patent No. 7,392,716; Piezoresistive strain concentrator, Washington, DC, U.S. Patent and Trademark Office.
6. T. Kwa, J. Letterneau, and R. Martin, "Resonance Modes of the High-Survivability, High-Shock Accelerometer," *Proc. SAVIAC 81st Shock and Vibration Symposium*, Orlando, FL, October 2010.
7. V. I. Bateman, F. A. Brown, and N. T. Davie, "The Use of a Beryllium Hopkinson Bar to Characterize a Piezoresistive Accelerometer in Shock Environments," *Journal of the Institute of Environmental Sciences*, Vol. XXXIX, No. 6, pp. 33-39, November/December 1996.
8. V. I. Bateman and J. Letterneau, "Characterization of Damped Accelerometers with Full Range Hopkinson Bar Shock," *Proc. of the 83rd Shock and Vibration Symposium*, New Orleans, LA, November, 2012 (paper) and ESTECH2013, San Diego, CA, May 2013.
9. V. I. Bateman, F. A. Brown, and M. A. Nusser, "High Shock, High Frequency Characteristics of a Mechanical Isolator for a Piezoresistive Accelerometer, the ENDEVCO 7270AM6," SAND00-1528, National Technical Information Service, 5285 Port Royal Road, Springfield, VA, July 2000.
10. Anon., *MIL-STD-810G Change Notice 1*: Environmental Engineering Considerations and Laboratory Tests, Method 516 for Shock, and Method 517 for Pyroshock, April 2014.
11. V. I. Bateman, "ISO 16063-22 Amendment," *Proc. SAVIAC 83rd Shock and Vibration Symposium*, New Orleans, LA, November 2012.
12. R. Davies, "A Critical Study of the Hopkinson Pressure Bar," *Philosophical Transactions*, Series A, Royal Society of London, V. 240, pp. 352-375, January 8, 1948.
13. H. Kolsky, *Stress Waves in Solids*, Oxford University Press, 1953.
14. V. I. Bateman, B. D. Hansche, and O. M. Solomon, "Use of a Laser Doppler Vibrometer for High-Frequency Accelerometer Characterizations," *Proc. of the 66th Shock and Vibration Symposium*, Vol. I, Biloxi, MS, November 1995.
15. ISO 16063-22:2005, "Methods for the calibration of vibration and shock transducers – Part 22: Shock calibration by comparison to a reference transducer."
16. S. D. Stearns, *Digital Signal Analysis*, pp. 37-40, Hayden Book Company Inc., 1975.
17. S. D. Stearns, "Integration and Interpolation of Sampled Waveforms," *SAND77-1643*, Sandia National Laboratories, January, 1978.
18. Bendat, J. S. and A. G. Piersol, Random Data, 2nd Edition, John Wiley and Sons, 1986, pp.164-185.

The author can be reached at: vilshock@comcast.net.